Journal of Magnetic Resonance 337 (2022) 107177

Contents lists available at ScienceDirect

Journal of Magnetic Resonance

journal homepage: www.elsevier.com/locate/jmr

Relaxation optimized double acquisition (RODA) as an alternative for virtual decoupling of NMR spectra

Alvar D. Gossert *, Gerhard Wider

Department of Biology, Biomolecular NMR Spectroscopy Platform, ETH Zürich, 8093 Zürich, Switzerland

ARTICLE INFO

Article history:
Received 9 January 2022
Accepted 23 February 2022
Available online 4 March 2022

Keywords:
Spin-state selection
Virtual decoupling
TROSY
Dissolution DNP
Double acquisition
IPAP

ABSTRACT

We introduce an alternative way for spin-state selection, RODA, which yields higher sensitivity for spin systems exhibiting a TROSY effect. With RODA, the TROSY component of a doublet is recorded twice using a double acquisition scheme. RODA works by simple addition of consecutive NMR signals, and does not require any special processing. Thus, this pulse sequence element can seamlessly be integrated into existing experiments. We demonstrate the broad applicability of RODA with several systems exhibiting a TROSY effect on ^{15}N–^{1}H, ^{19}F–^{13}C or ^{1}H–^{13}C moieties. Further, we show that virtual decoupling with increased sensitivity is possible in a single double acquisition experiment in situations as encountered with dissolution DNP.

1. Introduction

NMR signals are often split into multiplets due to scalar couplings. In order to collapse these multiplets into a single line and to obtain simplified spectra of higher intensity, decoupling pulse trains are typically applied during acquisition [1]. However, such decoupling is not always technically feasible or may even not be desired. For instance, homonuclear decoupling of a certain bandwidth during the acquisition is often not selective enough and interferes with the observed magnetization, like for example in ^{13}C carbonyl-detected experiments. A case where decoupling is not desired are spin pairs exhibiting cross correlated relaxation [2–5], *i.e.* a "TROSY-effect", such as ^{1}H and ^{15}N nuclei in amides or ^{13}C nuclei in ^{13}C–^{1}H [6] and ^{13}C-^{19}F spin pairs [7]. Decoupling would mix slow and fast relaxing components of the doublet leading to overall lower signal intensity and broadening of the resonance line.

For TROSY spectra exhibiting multiplets, several methods for spin-state selection (S^3) have therefore been devised for virtual decoupling. The two most prominent variants are IPAP (in-phase anti-phase [8,9]) and S^3E (spin-state selective excitation [10]). These techniques require different phases for the two doublet components. One component is kept in a pure absorptive mode in subsequent scans and the other component is phase shifted by 0° and 180° (IPAP) or ± 90° (S^3E). The phase difference is accomplished by delays depending on the scalar coupling $^{1}J_{IS}$ ($1/2J$ (IPAP) or $1/4J$ (S^3E)), during which scalar coupling evolution is active. Spectra with singlet lines can then spectroscopically be obtained by appropriate phase cycling, resulting in addition of the desired doublet component and subtraction of the undesired component. These procedures depend on homogeneous *J*-couplings of all signals and identical intensity of the signals in consecutive scans. With these conditions fulfilled, both approaches result in clean spectra with singlet signals.

As a disadvantage, these spin-state selection procedures discard the rejected doublet component completely, and therefore result in 2-fold lower sensitivity compared to pulsed decoupling during acquisition in systems without TROSY effect. A certain remedy offer data processing procedures, in which the two doublet components are separately processed and therewith also using the signal of the second doublet component. A final spectrum is generated by shifting of the sub-spectra by ± 0.5 *J*, such that the two doublet components add up, leading to up to double the signal intensity [11,12]. But noise adds as well and a maximal sensitivity gain of $\sqrt{2}$ can thus be obtained. In this communication we term these advanced processing methods for virtual decoupling S^3E+ and IPAP+ .

We introduce relaxation optimized double acquisition (RODA), an alternative way of spin-state selection based on S^3E. RODA uses sequential acquisition [13–15] of both individual components of a doublet (Fig. 1). In the first acquisition period, the first component

* Corresponding author.
E-mail address: alvar.gossert@biol.ethz.ch (A.D. Gossert).

https://doi.org/10.1016/j.jmr.2022.107177
1090-7807/

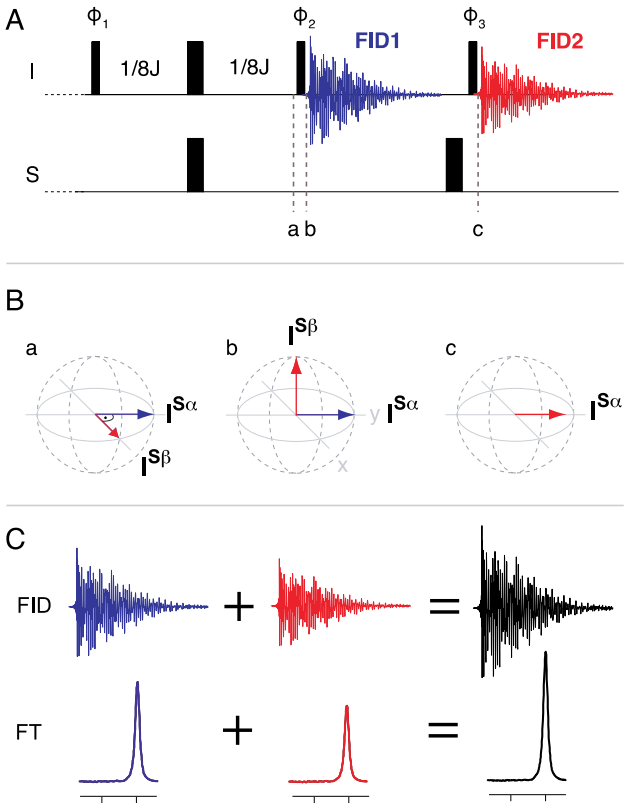

Fig. 1. Concept of relaxation optimized double acquisition (RODA). (A): Pulse sequence of the RODA element: narrow and wide rectangles represent 90° and 180° pulses, respectively, with their phases indicated above, if they differ from x = 0°. The first part of the sequence, up to point a, is identical to the S^3E element. The phase cycle for selecting the upfield component is φ_1 = 45°, 225°; φ_2 = 270°, 270°, 90°, 90°; φ_3 = 180°, 0°, 0°, 180°; φ_{rec} = 0°, 180°. For the downfield component, phases φ_1 and φ_2 need to be changed to: φ_1: 315°, 135°; φ_2: 90°, 90°, 270°, 270°. This phase cycle ensures storing the second component along the +z and –z-axis in alternating scans, such that effects arising from longitudinal relaxation during this period are cancelled. As shown in some examples, the basic pulse sequence can be modified (see also Suppl. Fig. 1): (i) for highest sensitivity, the second component can be stored along the +z-axis in every scan in order to exploit additional magnetization building up during the first acquisition period. To this end the phase cycle is reduced to φ_2: 270°, 90° and φ_3 = φ_{rec2} = 0°. (ii) For optimal suppression of the second component an alternating 180° pulse on S can be added prior to point a. (iii) For identical baselines in both scans or for water suppression, a spin echo can be added at point c. (B): Vector models for magnetization at points a, b and c of the pulse sequence. Here $I^{S\alpha}$ and $I^{S\beta}$ represent the TROSY and the anti-TROSY component of the I-spin, respectively. (C): Free induction decays FID1 (blue) and FID2 (red) can directly be added, resulting in the black signal after Fourier Transformation (FT). For visual clarity the individual Fourier transformed signals are shown below the respective FIDs. See main text for explanation of the exact procedure.

(*i.e.* the TROSY component) is recorded and the second (anti-TROSY) component is stored in a z-state. After recording the first FID (FID1), the coupled spins are inverted, effectively converting the stored anti-TROSY component into the TROSY component. The signal recorded during the second acquisition (FID2) stems from the same spectroscopic transition as the first one, and therefore has exactly the same chemical shift and the same relaxation properties as the first signal. Thus, the signals can be constructively added without any modifications. This represents a purely spectroscopic method for spin-state selection in a single scan (using double acquisition), which takes advantage of the entire available magnetization. In the following, we present several examples of applications of RODA and discuss the limitations and advantages of this approach.

2. Results

2.1 The RODA experiment

The RODA experiment is derived from the familiar S^3E element. In an I, S two-spin system we describe the two doublet components of the I spin by the state of the S spin, Sα and Sβ, respectively, *i.e.* $I^{S\alpha}$ and $I^{S\beta}$. The pulse sequence starts with a period of 1/4*J* during which the spin system evolves under *J*–coupling into an orthogonal state (Fig. 1, point a). Let $I^{S\alpha}$ be the TROSY-component and $I^{S\beta}$ the anti-TROSY component. The coherence can then be described as $I_y^{S\alpha}$ = ½ $I_y - I_yS_z$ and $I_x^{S\beta}$ = ½ $I_x + I_xS_z$. At this time, a 90° pulse is applied along the y-axis such that the anti-TROSY component is brought into a z-state (Fig. 1, point b). Immediately after this pulse at point b, a first free induction decay (FID1) is recorded, which yields a sharp TROSY-type signal. During acquisition of the FID1, the $I^{S\beta}$ (anti-TROSY) component is stored in a slowly relaxing superposition of I_z-S_z and I_z states and can subsequently be read out by a 90°$_x$ pulse (Fig. 1, point c). Inversion of the S spins at the same time allows again the observation of the desired doublet component with optimized transverse relaxation properties. The signals from the two FIDs can seamlessly be added since their resonance frequencies are identical (*i.e.* the one of the TROSY component) and no further processing is necessary as in advanced IPAP+ or S^3E+ experiments where phase or frequency shifts are required for instance.

The RODA pulse sequence as shown in Fig. 1 can be used directly to record a spin-state-selective 1D spectrum or it can be used as an element in a higher dimensional spectrum, e.g. in place of a refocusing INEPT. The RODA pulse sequence can start from in-phase (I_z) magnetization or two-spin order ($2I_zS_z$), and the same orthogonal spin state will be reached as at point a (Fig. 1). Therefore, RODA can be employed in a rather flexible manner as shown in various examples below.

2.2 Comparison of conventional and virtual decoupling approaches with (^{15}N)-^{1}H RODA

The performance of the different methods (conventional decoupling, S^3E, IPAP, S^3E+, IPAP+, (^{15}N)-^{1}H RODA) was measured on proteins with different rotational correlation times, τ_c, namely the small N-terminal domain of 434 repressor ($\tau_c \approx 4$ ns) and the membrane protein OmpX in detergent micelles at 30 °C and 10 °C ($\tau_c \approx 23$ ns and 40 ns, respectively, Fig. 2). For small proteins pulsed heteronuclear decoupling during acquisition leads to significantly higher signal intensity than any of the tested virtual decoupling methods (The IPAP data is not shown, as the results were essentially the same as for the S^3E method). With RODA the theoretical gain of $\sqrt{2}$ in sensitivity expected in the absence of a TROSY-effect, is not fully realized since the component stored during recording of the first FID, loses intensity due to longitudinal relaxation. For OmpX, RODA leads to higher signal intensity than decoupling or IPAP/S^3E(+) approaches (Fig. 2). When the intensity of the anti-TROSY component is lower than 0.4 (= $\sqrt{2}$–1) times the TROSY component, IPAP+ and S^3E+ will not increase the sensitivity since noise is increased by $\sqrt{2}$ when adding/subtracting shifted spectra. Since in RODA the anti-TROSY component only suffers transverse relaxation for a period of 1/4*J* (*i.e.* 2.7 ms for ^{15}N,^{1}H-moieties), a larger proportion of signal can be carried over to the second acquisition despite the (comparatively) small relaxation during the stored z-state, leading to an improved overall sensitivity.

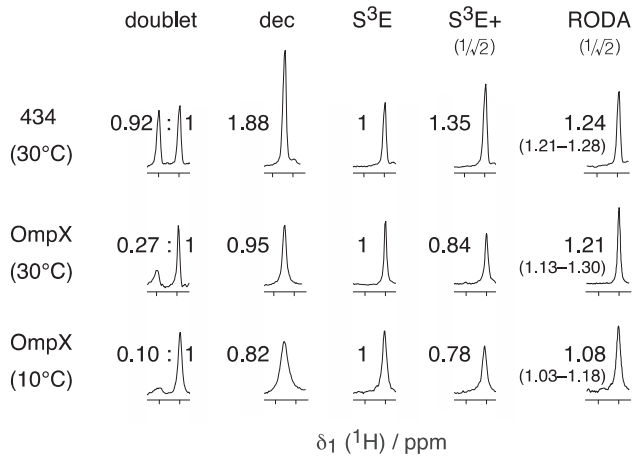

Fig. 2. Excerpts of 1D ^{1}H spectra obtained with different types of ^{15}N-decoupling, namely a conventional half-filter without (doublet) and with (dec) ^{15}N-decoupling during acquisition; spin-state-selective excitation (S^3E); S^3E with advanced processing including the second component (S^3E+) and relaxation optimized double acquisition (RODA). Isolated signals are shown, obtained from proteins of different rotational correlation times (τ_c): (^{13}C,^{15}N)-434 repressor (1–63), τ_c(30 °C) ≈ 4 ns; [80% ^{2}H,^{15}N]-OmpX in protonated DHPC, τ_c(30 °C) ≈ 23 ns, τ_c(10 °C) ≈ 40 ns [16]. The average relative signal-to-noise ratio with reference to the S^3E signal of the same sample is given by the number next to the peak. Where deviations of more than 5% from the average value were observed among all signals, the range of values is indicated in parenthesis below. The S^3E+ and RODA spectra were divided by a factor of $\sqrt{2}$ for normalization of the noise level. The spectra were obtained on a Bruker DRX 750 MHz spectrometer equipped with a triple resonance probe with a shielded z-gradient coil.

2.3 Example: 2D [^{1}H,^{1}H]-NOESY spectra with ^{15}N editing – (^{15}N)-^{1}H RODA yields narrower signals with higher intensity than conventional decoupling

In Fig. 3, an application of RODA in conjunction with a half-filter element as an ^{15}N-editing module in the direct dimension of a 2D [^{1}H,^{1}H]-NOESY experiment is shown (see supplement for details on the pulse sequence). The sample was (80% ^{2}H, u-^{15}N)-labelled OmpX in protonated DHPC micelles at 10 °C, a system equivalent to a particle of 100 kDa at room temperature. The comparison with a conventional half-filter experiment with ^{15}N decoupling reveals sharper lines of up to 1.4 times higher intensity for the RODA version (Fig. 3). For perdeuterated biomolecules an even more important enhancement can be expected, since z-state relaxation of the second component should be further reduced during the acquisition of the first one.

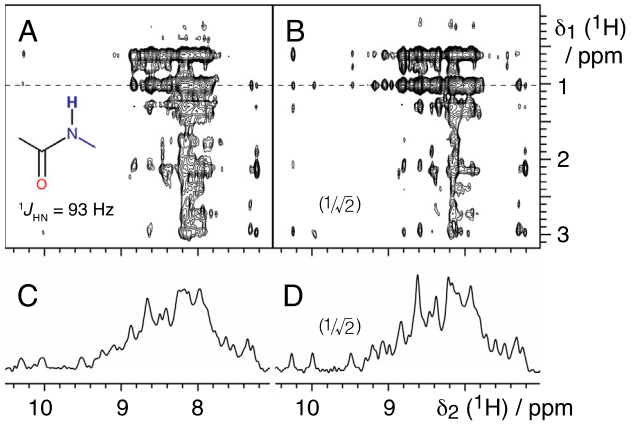

Fig. 3. 2D [^{1}H,^{1}H]-NOESY spectra with ^{15}N editing in δ_2 with either decoupling (A) or RODA (B). In (C) and (D), 1D slices, taken at the dashed line in the 2D spectra are shown, representing intermolecular NOEs between protein and detergent molecules of the surrounding micelle. Spectra B and D were divided by a factor of $\sqrt{2}$ for normalization of the noise level. The spectra were recorded with a NOESY mixing time of = 250 ms at 10 °C on a Bruker DRX 750 MHz spectrometer, equipped with a triple resonance TXI probe. The sample consisted of 0.4 mM 80% ^{2}H,^{15}N labelled OmpX in protonated 1,2-dihexanoyl-glycero-3-phosphocholine (DHPC) micelles.

For this particular experiment the basic RODA pulse sequence was modified in two ways (Suppl. Fig. 1). In order to suppress the anti-TROSY component completely, an additional 90°$_x$-180°$_y$-90°$_x$ composite pulse on ^{15}N was introduced prior to point a in Fig. 1. Alternating the phase of the second 90° pulse in this element between +x and –x (effectively inverting the ^{15}N spins or not) leads to a +/– 90° phase shift of the anti-TROSY component relative to the in-phase TROSY component, resulting in optimal cancellation of the anti-TROSY component. In filtered/edited NOESY experiments, suppression of artefacts is essential since weak NOE peaks should be identified, hence this additional 180° composite pulse.

The second modification is the introduction of a WATERGATE [17] element in both sub-scans for water suppression (Suppl. Fig. 1).

2.4 Example: aromatic [^{19}F,^{13}C] TROSY – (^{19}F)-^{13}C RODA yields increased sensitivity in 1D spectra

In carbon detected spectroscopy, two important TROSY effects can be exploited in ^{19}F–^{13}C- and in ^{1}H–^{13}C-moieties in aromatic residues [6,7]. In both cases the TROSY effect is highly pronounced on the carbon nucleus, but there is little interference of relaxation effects on the partner nucleus ^{1}H or ^{19}F.

The optimal use of RODA in this context is in 1D ^{13}C-detected experiments. We first turned our attention to the recently exploited ^{19}F,^{13}C-TROSY effect [7,18–20]. Interestingly, for two of three observable signals in the ^{19}F,^{13}C-Tyr-labeled GB1 sample, the 1D ^{13}C experiment was more sensitive than the counterpart starting with ^{19}F magnetization. Relaxation effects on ^{19}F, most probably due to exchange broadening, led to strong attenuation of these signals. For 1D ^{13}C experiments the RODA scheme shows 1.3-fold superior sensitivity over the conventional IPAP scheme and 1.2-fold higher sensitivity than the advanced IPAP+ processing (Fig. 4).

For the 2D [^{19}F,^{13}C]-TROSY experiment it was shown that the most sensitive spectra were obtained with carbon detection [7], as accomplished with a single transition to single transition polarization transfer (ST2-PT [21,22]) for selection of the TROSY component. In this way sensitivity-enhanced, phase-modulated 2D spectra can be obtained [23,24]. RODA is not compatible with phase encoding of the indirect dimension and therefore a conventional refocused INEPT sequence [25] was used for obtaining 2D-[^{19}F,^{13}C] correlations. This RODA approach was always less sensitive than the ST2-PT sequence due to the sensitivity enhancement of the latter and the optimal use of steady-state ^{13}C–magnetization (data not shown).

2.5 Example: 2D [^{1}H,^{13}C] aromatic TROSY spectra of uniformly ^{13}C-labeled proteins – RODA yields improved sensitivity and suppresses coupling artefacts

2D-[^{1}H,^{13}C] aromatic TROSY spectra are usually recorded on uniformly ^{13}C labeled samples. Thus, homonuclear carbon–carbon couplings with sizeable $^{1}J_{CC}$ values of 56–60 Hz lead to splitting of the signals and to phase-distorted line shapes in ST2-PT-based spectra. These distortions can usually only be overcome by sparse isotope labeling approaches [26]. The corresponding RODA pulse sequence (Suppl. Fig. 2) requires only half the duration of the ST2-PT element on the detected carbon, such that less phase differences evolve during the refocusing INEPT step. Additionally, RODA has an inherent correction, due to the 90° pulse immediately prior

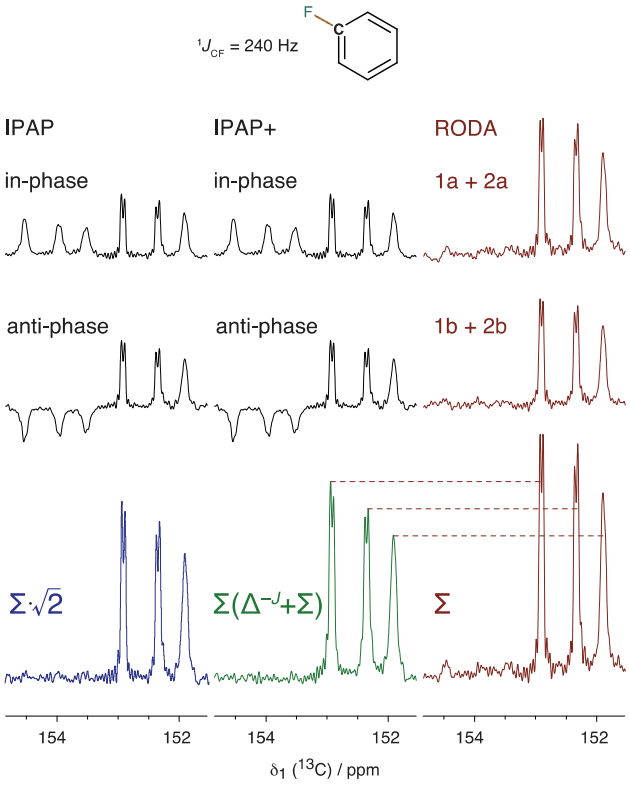

Fig. 4. Comparison of 1D ^{13}C spectra of 1 mM 3-^{19}F,^{13}C-tyrosine labeled GB1 with spin-state selection based on IPAP (black) and RODA (red). For IPAP, signals of 512 scans each were stored separately to obtain in-phase and anti-phase spectra. Two types of spectra were obtained from this data: simple summing up of the in-phase and anti-phase spectra resulted in the blue spectrum (IPAP). The green spectrum was obtained in two processing steps: (i) addition and subtraction of the two datasets above and (ii) addition of the resulting datasets after shifting of the difference spectrum by $-^1J_{FC}$ (IPAP+). For RODA, 512 double-scans were recorded and signals of the first scan (FIDs 1a and 2a) and the second scan (FIDs 1b and 2b) were stored separately. Simple addition of the corresponding (1a + 2a and 2a + 2b, respectively) spectra yielded the final spectrum (Σ). In order to obtain an identical noise level for all resulting spectra, the blue spectrum was multiplied by 1.41, as the other spectra resulted from the addition of four spectra and the blue only of two spectra. RODA spectra (a) and (b) are the result of double the number of FIDs, since two FIDs are acquired in RODA during the time of one scan in IPAP. The blue and red spectra can directly be obtained spectroscopically by signal summation, while for the green spectrum a special processing procedure is required. Spectra were recorded in 37 min (IPAP) and 40 min (RODA) at 4 °C on a 600 MHz Bruker Avance IIIHD spectrometer equipped with a QCI-F CryoProbe™.

to acquisition [27]. Therefore, phase distortions are nearly absent, leading to cleaner 2D-[^{1}H,^{13}C] spectra with higher intensity (Fig. 5).

2.6 Example: virtual decoupling in a single double acquisition in e.g. dissolution DNP experiments

RODA allows obtaining singlet spectra without the necessity of phase cycling and is not affected by different signal intensities in two consecutive scans. Thus, it offers itself as an alternative to homonuclear decoupling e.g. in dissolution DNP experiments, where the hyperpolarized signal decays fast and doesn't permit phase cycling [28–32]. In lack of a dissolution DNP setup, we used a highly concentrated sample of 0.5 M 2,3-^{13}C-labeled pyruvate to test virtual decoupling in a single double acquisition of a homonuclear 1D ^{13}C experiment (Fig. 6). To make the analogy to the heteronuclear RODA experiment in Fig. 1 the methyl carbon represents the I-spin and the carbonyl carbon the S-spin and the hard rf pulses are replaced by selective pulses at the resonance frequency of these I- and S-spins. In the resulting spectra suppression of the

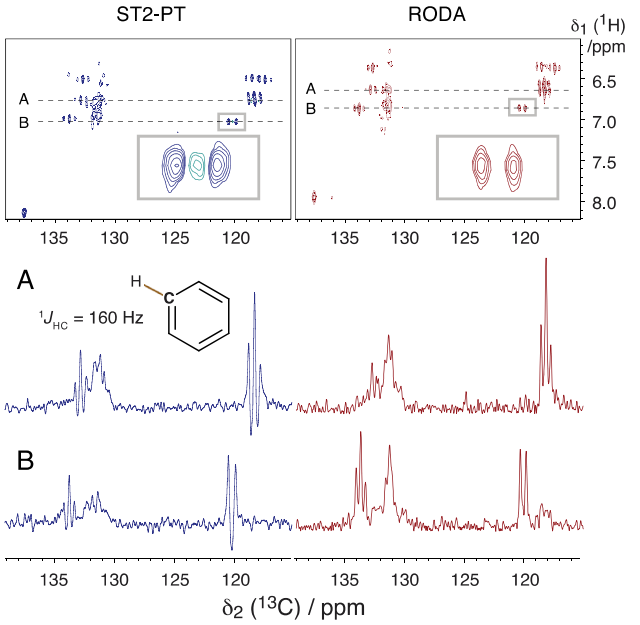

Fig. 5. Aromatic 2D [^{1}H,^{13}C]-TROSY spectra recorded with ST2-PT (left) and RODA (right). In the ST2-PT spectrum the downfield component of ^{1}H and the upfield (TROSY-) component of ^{13}C were selected. Spectra selecting the upfield component of ^{1}H yielded the same sensitivity (not shown). In the RODA spectrum the upfield component of ^{13}C was selected and ^{1}H was decoupled in the indirect dimension (hence the shift in the ^{1}H dimension). In (A) and (B), 1D ^{13}C slices of the 2D spectrum above are shown, taken at the positions indicated by the respective dashed lines in the 2D spectra. The RODA sequence yields purely absorptive line shapes as seen in the magnified signals in the 2D spectrum (grey boxes) and in the 1D slices. The shorter spin echo delays lead to higher sensitivity especially on triplet signals and the 90° pulse immediately prior to acquisition eliminates phase distortions. Spectra were recorded in 2 h 30 min (ST2-PT) and 2 h 42 min (RODA) using 32 scans (or double-scans) and 128 complex points in the indirect dimension. The experiments were performed at 25 °C on a 600 MHz Bruker Avance IIIHD spectrometer equipped with a QCI-F CryoProbe™. The sample was a 2.8 mM solution of uniformly ^{13}C,^{15}N-labeled protein 1290 of *thermatoga maritima*.

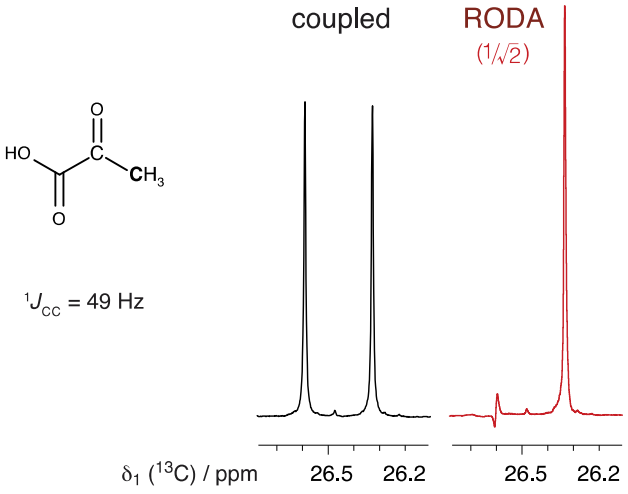

Fig. 6. 1D ^{13}C spectrum obtained from a single acquisition using conventional (coupled, black) or RODA (red) experiments. Signals of the methyl (3) group of a 0.5 M sample of 2,3-^{13}C-labeled pyruvate are shown. A proton decoupled one-pulse ^{13}C experiment yields the black spectrum, and the RODA sequence yields the red spectrum. The RODA spectrum was divided by $\sqrt{2}$ in order to obtain the same noise level. Spectra were acquired on a Bruker 600 MHz AVNEO spectrometer equipped with a triple resonance TCI CryoProbe, using an acquisition time of 1.1 s. Band-selective pulses of the Q5 sebop (350 us) and Q3 surop (270 µs) kind [33], both with approx. 8 kHz excitation bandwidth as implemented in the Bruker library, were used for selective excitation and inversion of methyl and carbonyl nuclei.

second doublet component is not perfect, but it is reduced to less than 10% compared to the selected component (5–7% in the shown experiments). A gain in sensitivity of 1.31 was obtained, irrespective of whether the second component was stored along the +z or –z-axis during acquisition of the first one, reflecting the slow T_1 relaxation of these ^{13}C nuclei. Therefore, a similar gain should be achieved under hyperpolarized conditions.

3. Discussion

We presented a novel way of recording TROSY spectra using S^3E-type spin-state selection and acquisition of both doublet components. Compared to advanced S^3E + and IPAP + procedures, in RODA the signal of the anti-TROSY component is not acquired in its unfavorable anti-TROSY state, but it is converted into the TROSY component, such that two highly sensitive spectra with sharp and intense lines are obtained.

3.1 Relaxation optimized double acquisition

RODA relies on double acquisition, also termed queued acquisition, a concept which has been used in other contexts [14,15]. A very similar approach was used in qTROSY [13], where the anti-TROSY component on ^{15}N was stored for a second acquisition. There, however, no significant gain in sensitivity could be achieved, since the NMR experiment required extra delays and additional pulses, which abrogated the potential gains. In RODA, the pulse sequence is actually shortened compared to IPAP or ST2-PT spin-state selection procedures, therefore often resulting in increased sensitivity.

We showed applications to various systems exhibiting a TROSY effect, namely amide ^{15}N–^{1}H, aromatic ^{19}F-^{13}C and aromatic ^{1}H–^{13}C moieties on proteins of different size. On average roughly a gain in sensitivity of 1.2 is realized, compared to S^3E+ (Fig. 2) or IPAP + methods (Fig. 4). The established experiments would therefore need to be recorded for a 50% longer time than the respective RODA version.

As shown, the RODA pulse sequence turns out to be quite versatile and rather generally applicable. Nevertheless, individual applications might require adaptation of the basic RODA pulse sequence. The adaptations we implemented shall be discussed in the following paragraphs.

3.2 Obtaining identical baselines in both sub-scans

With regards to the baseline one has to consider that in the first scan, the signal is read out after a spin echo, in the second scan the signal is recorded after a single 90° pulse. This can lead to slightly different baselines in the two sub-scans. In this situation a short spin echo sequence consisting of a 180° and a 90° pulse along the y-axis can be added at point c in Fig. 1 to obtain identical baselines in both scans. When recording proton spectra in aqueous solution without presaturation, water suppression elements must be added to both sub-scans (Suppl. Fig. 1)

3.3 Optimal suppression of second doublet component

A residual anti-TROSY component can be present in the first and the second sub-scan for different reasons. In the first sub-scan, imperfections in the 1/8*J* delay and the final 90° pulse, which should flip the anti-TROSY component entirely along the z-axis, may lead to a spurious dispersive signal. This artefact can be effectively suppressed by adding alternating 0°/ 180° pulses on the S-spins at point a in Fig. 1. This leads to a +/– 90° phase shift of the anti-TROSY component relative to the in-phase TROSY component in alternate scans, resulting in optimal cancellation of the anti-TROSY component in the first scan.

The reason for artefacts in the second sub-scan, is that an anti-TROSY component can build up during the first acquisition period due to T_1 relaxation, leading to a small absorptive signal. This signal is efficiently suppressed by storing the second component alternatively in a + or – z state during the acquisition of the first FID by virtue of a phase cycle as implemented in the basic RODA sequence (φ_2 in Fig. 1A).

However, storing the second component along the –z axis leads to a slight reduction in signal intensity due to different T_1 relaxation.

On the other hand, in situations with limited sensitivity, and a certain tolerance against spurious signals of the second component, T_1 relaxation should be exploited in order to restore some of the magnetization lost during the first part of the pulse sequence. Especially in situations with a broad anti-TROSY signal, this strategy does not seem to introduce visible artefacts and leads to an increased sensitivity of a few percent (Fig. 4).

3.4 Considerations on the optimal acquisition time in RODA

In RODA experiments the acquisition time needs to be optimized at the time of recording, unlike in conventional experiments where this could often be deferred to the processing step. In double acquisition experiments long acquisition times will lead to reduced intensities in the second sub-scan due to more T_1 relaxation during the first acquisition. Further, the intensity of the unwanted anti-TROSY component is increased.

For the protein samples studied here, the natural linewidth of the TROSY component was always larger than 10 Hz, such that we chose an acquisition time of 0.1 s for these systems, which also reflects the signal-to-noise optimum in conventional experiments. For the small molecule pyruvate with an experimental linewidth of 1 Hz, an acquisition time of 1 s was chosen.

3.5 Absorptive line shapes in aromatic [^{1}H,^{13}C]-TROSY

For aromatic 2D [^{1}H,^{13}C]-TROSY spectra, typically recorded on uniformly ^{13}C labeled samples, the RODA version has a welcomed side effect: the short refocusing INEPT delay and the 90° pulse prior to acquisition lead to a spectrum with clean absorptive line shapes (Fig. 5). The artefacts due to large homonuclear $^{1}J_{CC}$ couplings in the aromatic systems are less pronounced and are purged by the 90° pulse, which acts in the same way as in perfect echo sequences [27]. The striking improvement in spectral quality suggests exploiting the perfect echo in biomolecular ^{13}C spectroscopy. Several applications along these lines will be published elsewhere.

3.6 RODA as an alternative for virtual decoupling

For many practical purposes, virtual decoupling can be achieved for two-spin systems by IPAP or S^3E techniques in a satisfactory way. RODA can be used as an alternative, which works by simple summation of scans and does not require processing of separate sub-spectra and their recombination. For systems without pronounced TROSY effect, the sensitivity of RODA is in between the one of conventional IPAP/S3E and IPAP+/S3E + with advanced processing. The second component in RODA will always yield less intensity than the first one, due to relaxation of the z-state during the recording of the first component. Typically, 70–80% of the intensity of the first scan can be obtained for systems without TROSY effect. Since the second scan adds noise, a maximal sensitivity gain of $\sim$ 1.3 can be obtained, compared to 1.4 in the case of advanced IPAP + . (The estimate of 1.3 is based on the extensive

phase cycle of φ_2 producing a clean spectrum. Higher sensitivity can be obtained by omitting this phase cycle, as discussed above).

Where RODA stands out among the methods for virtual decoupling is in situations where only one scan can be acquired or where consecutive scans don't have the same signal intensity. This is for example the case in hyperpolarization experiments [28].

4. Conclusion

In summary, RODA is a concept that can be used as module for acquisition of a single component of a doublet signal in a wide variety of experiments. It shows significantly higher sensitivity in 1D TROSY-type spectra compared to established methods, because the fast-relaxing anti-TROSY component is converted into the slowly relaxing one before recording it, leading to narrow and intense resonance lines.

For 2D spectra correlating both nuclei of a TROSY spin-pair, the ST2-PT scheme is superior to RODA due to sensitivity enhancement and optimal use of steady-state magnetization. In cases were simple selection of the TROSY component is required (Fig. 3) or sizeable homonuclear couplings are present (Fig. 5), RODA is superior.

For virtual decoupling of spin systems without TROSY effect, the sensitivity of RODA is up to 1.3-fold higher than conventional IPAP or S^3E, but lower than IPAP + or S^3E + -type spectra with advanced processing. However, the latter require somewhat involved processing including shifting of spectra, while RODA works at the level of simply adding up FIDs without additional processing. Further, IPAP and S^3E rely on subtraction of signals and therefore require identical signal intensities in consecutive scans. RODA, in contrast, is robust against different intensities in consecutive scans and therefore has an additional field of application in situations with non-steady-state magnetization, e.g. in hyperpolarized experiments.

Declaration of Competing Interest

The authors declare that they have no known competing financial interests or personal relationships that could have appeared to influence the work reported in this paper.

Acknowledgements

First and foremost, we would like to thank Kurt Wüthrich for having provided such a stimulating research atmosphere and first in class training in his research group at ETH Zürich, of which the authors had the privilege to be part of.

We would like to thank Helena Kovacs for help with ^{19}F,^{13}C TROSY spectra, and Haribabu Arthanari and Andras Boeszoermenyi for generously allowing us to use an old GB1 sample. Christian Hilty, Fred Damberger, Neel Sarovar Bhavesh and Touraj Etezady-Esfarjani are thanked for protein samples and plasmid DNA. Finally, we would like to thank Simon Rüdisser for valuable discussions. This work was funded by ETH Zürich.

Appendix A. Supplementary material

Supplementary data to this article can be found online at https://doi.org/10.1016/j.jmr.2022.107177.

References

[1] A.J. Shaka, J. Keeler, Broadband spin decoupling in isotropic liquids, Prog. Nucl. Magn. Reson. Spectrosc. 19 (1987) 47–129, https://doi.org/10.1016/0079-6565(87)80008-0.

[2] K. Pervushin, Impact of transverse relaxation optimized spectroscopy (TROSY) on NMR as a technique in structural biology, Q. Rev. Biophys. 33 (2000) 161–197, https://doi.org/10.1017/S0033583500003619.

[3] K. Pervushin, R. Riek, G. Wider, K. Wüthrich, Attenuated T_2 relaxation by mutual cancellation of dipole–dipole coupling and chemical shift anisotropy indicates an avenue to NMR structures of very large biological macromolecules in solution, Proc. Natl. Acad. Sci. 94 (1997) 12366–12371, https://doi.org/10.1073/pnas.94.23.12366.

[4] M. Goldman, Interference Effects in the Relaxation of a Pair of Unlike Spin-1/2 Nuclei, J. Magn. Reson. 60 (1984) (1969) 437–452, https://doi.org/10.1016/0022-2364(84)90055-6.

[5] J. Boyd, U. Hommel, I.D. Campbell, Influence of cross-correlation between dipolar and anisotropic chemical shift relaxation mechanisms upon longitudinal relaxation rates of ^{15}N in macromolecules, Chem. Phys. Lett. 175 (1990) 477–482, https://doi.org/10.1016/0009-2614(90)85567-V.

[6] K. Pervushin, R. Riek, G. Wider, K. Wüthrich, Transverse Relaxation-Optimized Spectroscopy (TROSY) for NMR Studies of Aromatic Spin Systems in ^{13}C-Labeled Proteins, J. Am. Chem. Soc. 120 (1998) 6394–6400, https://doi.org/10.1021/ja980742g.

[7] A. Boeszoermenyi, S. Chhabra, A. Dubey, D.L. Radeva, N.T. Burdzhiev, C.D. Chanev, O.I. Petrov, V.M. Gelev, M. Zhang, C. Anklin, H. Kovacs, G. Wagner, I. Kuprov, K. Takeuchi, H. Arthanari, Aromatic ^{19}F–^{13}C TROSY: a background-free approach to probe biomolecular structure, function, and dynamics, Nat Methods. 16 (2019) 333–340, https://doi.org/10.1038/s41592-019-0334-x.

[8] M. Ottiger, F. Delaglio, A. Bax, Measurement of J and Dipolar Couplings from Simplified Two-Dimensional NMR Spectra, J. Magn. Reson. 131 (1998) 373–378, https://doi.org/10.1006/jmre.1998.1361.

[9] P. Andersson, J. Weigelt, G. Otting, Spin-state selection filters for the measurement of heteronuclear one-bond coupling constants, J. Biomol. NMR 12 (1998) 435–441, https://doi.org/10.1073/pnas.94.23.12366.

[10] A. Meissner, J.Ø. Duus, O.W. Sørensen, S.-S.-S. Excitation, Application for E. COSY-Type Measurement of J_{HH} Coupling Constants, J. Magn. Reson. 128 (1997) 92–97, https://doi.org/10.1006/jmre.1997.1213.

[11] N.C. Nielsen, H. Thogersen, O.W. Sørensen, Doubling the Sensitivity of INADEQUATE for Tracing Out the Carbon Skeleton of Molecules by NMR, J. Am. Chem. Soc. 117 (1995) 11365–11366, https://doi.org/10.1021/ja00150a045.

[12] W. Bermel, I. Bertini, I. Felli, M. Piccioli, R. Pierattelli, ^{13}C-detected protonless NMR spectroscopy of proteins in solution, Prog. Nucl. Magn. Reson. Spectrosc. 48 (2006) 25–45, https://doi.org/10.1016/j.pnmrs.2005.09.002.

[13] T. Diercks, V.Y. Orekhov, qTROSY – a novel scheme for recovery of the anti-TROSY magnetisation, J. Biomol. NMR 32 (2005) 113–127, https://doi.org/10.1007/s10858-005-5618-z.

[14] C. Dalvit, A.D. Gossert, J. Coutant, M. Piotto, Rapid acquisition of ^1H and ^{19}F NMR experiments for direct and competition ligand-based screening, Magn. Reson. Chem. 49 (2011) 199–202, https://doi.org/10.1002/mrc.2733.

[15] A.D. Gossert, C. Henry, M.J.J. Blommers, W. Jahnke, C. Fernández, Time efficient detection of protein-ligand interactions with the polarization optimized PO-WaterLOGSY NMR experiment, J Biomol NMR. 43 (2009) 211–217, https://doi.org/10.1007/s10858-009-9303-5.

[16] D. Lee, C. Hilty, G. Wider, K. Wüthrich, Effective rotational correlation times of proteins from NMR relaxation interference, J. Magn. Reson. 178 (2006) 72–76, https://doi.org/10.1016/j.jmr.2005.08.014.

[17] M. Liu, X. Mao, C. Ye, H. Huang, J.K. Nicholson, J.C. Lindon, Improved WATERGATE pulse sequences for solvent suppression in NMR spectroscopy, J. Magn. Reson. 132 (1998) 125–129.

[18] O.B. Becette, G. Zong, B. Chen, K.M. Taiwo, D.A. Case, T.K. Dayie, Solution NMR readily reveals distinct structural folds and interactions in doubly ^{13}C- and ^{19}F-labeled RNAs, Sci. Adv. 6 (2020) eabc6572, https://doi.org/10.1126/sciadv.abc6572.

[19] A. Divakaran, S.E. Kirberger, W.C.K. Pomerantz, SAR by (Protein-Observed) ^{19}F NMR, Acc. Chem. Res. 52 (2019) 3407–3418, https://doi.org/10.1021/acs.accounts.9b00377.

[20] F. Nußbaumer, R. Plangger, M. Roeck, C. Kreutz, Aromatic ^{19}F–^{13}C TROSY — [^{19}F, ^{13}C]-Pyrimidine Labeling for NMR Spectroscopy of RNA, Angew. Chem. 132 (2020) 17210–17217, https://doi.org/10.1002/ange.202006577.

[21] K.V. Pervushin, G. Wider, K. Wüthrich, Single Transition-to-single Transition Polarization Transfer (ST2-PT) in [^{15}N,^1H]-TROSY, J. Biomol. NMR 12 (1998) 345–348, https://doi.org/10.1023/A:1008268930690.

[22] K. Takeuchi, H. Arthanari, I. Shimada, G. Wagner, Nitrogen detected TROSY at high field yields high resolution and sensitivity for protein NMR, J Biomol NMR. 63 (2015) 323–331, https://doi.org/10.1007/s10858-015-9991-y.

[23] L. Kay, P. Keifer, T. Saarinen, Pure absorption gradient enhanced heteronuclear single quantum correlation spectroscopy with improved sensitivity, J. Am. Chem. Soc. 114 (1992) 10663–10665, https://doi.org/10.1021/ja00052a088.

[24] J. Cavanagh, A.G. Palmer III, P.E. Wright, M. Rance, Sensitivity improvement in proton-detected two-dimensional heteronuclear relay spectroscopy, J. Magn. Reson. 91 (1991) (1969) 429–436, https://doi.org/10.1016/0022-2364(91)90209-C.

[25] D.P. Burum, R.R. Ernst, Net polarization transfer via a *J*-ordered state for signal enhancement of low-sensitivity nuclei, J. Magn. Reson. 39 (1980) (1969) 163–168, https://doi.org/10.1016/0022-2364(80)90168-7.

[26] A.G. Milbradt, H. Arthanari, K. Takeuchi, A. Boeszoermenyi, F. Hagn, G. Wagner, Increased resolution of aromatic cross peaks using alternate ^{13}C labeling and TROSY, J Biomol NMR. 62 (2015) 291–301, https://doi.org/10.1007/s10858-015-9944-5.

[27] J.A. Aguilar, M. Nilsson, G. Bodenhausen, G.A. Morris, Spin echo NMR spectra without J modulation, Chem. Commun. 48 (2012) 811, https://doi.org/10.1039/c1cc16699a.

[28] J.H. Ardenkjaer-Larsen, B. Fridlund, A. Gram, G. Hansson, L. Hansson, M.H. Lerche, R. Servin, M. Thaning, K. Golman, Increase in signal-to-noise ratio of > 10,000 times in liquid-state NMR, Proc. Natl. Acad. Sci. 100 (2003) 10158–10163, https://doi.org/10.1073/pnas.1733835100.
[29] S. Jannin, A. Bornet, R. Melzi, G. Bodenhausen, High field dynamic nuclear polarization at 6.7 T: Carbon-13 polarization above 70% within 20 min, Chem. Phys. Lett. 549 (2012) 99–102, https://doi.org/10.1016/j.cplett.2012.08.017.
[30] A. Comment, Dissolution DNP for in vivo preclinical studies, J. Magn. Reson. 264 (2016) 39–48, https://doi.org/10.1016/j.jmr.2015.12.027.
[31] S. Chinthalapalli, A. Bornet, D. Carnevale, S. Jannin, G. Bodenhausen, Homonuclear decoupling for spectral simplification of carbon-13 enriched molecules in solution-state NMR enhanced by dissolution DNP, Phys. Chem. Chem. Phys. 18 (2016) 11480–11487, https://doi.org/10.1039/C5CP07884A.
[32] M. Ragavan, L.I. Iconaru, C. Park, R.W. Kriwacki, C. Hilty, Real-Time Analysis of Folding upon Binding of a Disordered Protein by Using Dissolution DNP NMR Spectroscopy, Angew. Chem. Int. Ed. 56 (2017) 7070–7073, https://doi.org/10.1002/anie.201700464.
[33] L. Emsley, G. Bodenhausen, Gaussian pulse cascades: New analytical functions for rectangular selective inversion and in-phase excitation in NMR, Chem. Phys. Lett. 165 (1990) 469–476, https://doi.org/10.1016/0009-2614(90)87025-M.